CFAR Matched Direction Detector

Olivier Besson, *Senior Member, IEEE,* and
Louis L. Scharf, *Fellow, IEEE*

***Abstract*—In a previously published paper by Besson *et al.*, we considered the problem of detecting a signal whose associated spatial signature is known to lie in a given linear subspace, in the presence of subspace interference and broadband noise of known level. We extend these results to the case of unknown noise level. More precisely, we derive the generalized-likelihood ratio test (GLRT) for this problem, which provides a constant false-alarm rate (CFAR) detector. It is shown that the GLRT involves the largest eigenvalue and the trace of complex Wishart matrices. The distribution of the GLRT is derived under the null hypothesis. Numerical simulations illustrate its performance and provide a comparison with the GLRT when the noise level is known.**

***Index Terms*—Array processing, detection, eigenvalues, Wishart matrices.**

I. Problem Statement

Detecting a signal in the presence of low-rank interference and broadband noise is an ubiquitous task in many array processing applications [2]. In the single-snapshot case, this problem has been studied in depth in [3], resulting in the so-called matched subspace detectors (MSDs). Adaptive versions of the MSD have been proposed and analyzed in [4] and references therein. In a recent paper [1], we considered the problem of detecting a signal whose steering vector is unknown, but known to lie in a subspace, using multiple snapshots from an array of sensors. More precisely, we used the following model for the L-dimensional received signal:

$$\begin{aligned} \boldsymbol{y}(t) &= \boldsymbol{a}s(t) + \boldsymbol{A}\boldsymbol{u}(t) + \boldsymbol{n}(t) \\ \boldsymbol{a} &= \boldsymbol{H}\boldsymbol{\theta}. \end{aligned} \tag{1}$$

In (1), $\boldsymbol{a} \in \mathbb{C}^L$ is the unknown steering vector, which belongs to the p-dimensional subspace $\langle \boldsymbol{H} \rangle$ spanned by the columns of $\boldsymbol{H} \in \mathbb{C}^{L\times p}$. In other words, $\boldsymbol{a}$ lies in a known subspace, but its orientation in $\langle \boldsymbol{H} \rangle$ is unknown. This modeling is relevant in a number of applications (see the discussion in [1]), where there exists some uncertainty about the steering vector of interest. The columns of $\boldsymbol{A} \in \mathbb{C}^{L\times J}$ form the J-dimensional interference subspace $\langle \boldsymbol{A} \rangle$ and $\boldsymbol{u}(t)$ denotes the interference waveforms. Finally, $\boldsymbol{n}(t)$ is a zero-mean complex-valued Gaussian noise with covariance matrix $\sigma^2\boldsymbol{I}$. In contrast to [1], where σ^2 was assumed to be known, we consider it to be *unknown* in the present correspondence.

As in [1], we assume that $\boldsymbol{H}$ and $\boldsymbol{A}$ are known full-rank matrices, and that the subspaces $\langle \boldsymbol{H} \rangle$ and $\langle \boldsymbol{A} \rangle$ are linearly independent. This implies that no element of $\langle \boldsymbol{H} \rangle$ can be written as a linear combination of vectors in $\langle \boldsymbol{A} \rangle$, and that the composite matrix $[\boldsymbol{H} \quad \boldsymbol{A}]$ is full rank. It is also assumed that $s(t)$ and $\boldsymbol{u}(t)$ are deterministic sequences, as in [1]. Note that a stochastic framework could have been adopted, e.g., by assuming that $s(t)$ or/and $\boldsymbol{u}(t)$ are Gaussian random. This would lead to four possible models, each with a different generalized-likelood ratio test (GLRT). However, as observed in [5], these detectors would be approximately equivalent when the interference-to-noise ratio is large.

Manuscript received February 1, 2005; revised September 5, 2005. The work of L. L. Scharf is supported by the Office of Naval Research under Contract N00014-01-1-1019. The associate editor coordinating the review of this manuscript and approving it for publication was Dr. Sven Nordebo.

O. Besson is with the Department of Avionics and Systems, ENSICA, 31056 Toulouse, France.

L. L. Scharf is with the Departments of ECE and Statistics, Colorado State University, Fort Collins, CO 80523-1373 USA.

Digital Object Identifier 10.1109/TSP.2006.874782

II. Generalized-Likelihood Ratio Test

Our problem consists of deciding between the two hypotheses

$$\begin{cases} H_0: & \boldsymbol{Y} = \boldsymbol{A}\boldsymbol{U} + \boldsymbol{N} \\ H_1: & \boldsymbol{Y} = \boldsymbol{H}\boldsymbol{\theta}\boldsymbol{s}^T + \boldsymbol{A}\boldsymbol{U} + \boldsymbol{N} \end{cases} \tag{2}$$

where $\boldsymbol{Y} = [\boldsymbol{y}(1) \quad \cdots \quad \boldsymbol{y}(N)]$, $\boldsymbol{s} = [s(1) \quad \cdots \quad s(N)]^T$, $\boldsymbol{U} = [\boldsymbol{u}(1) \quad \cdots \quad \boldsymbol{u}(N)]$, and $\boldsymbol{N} = [\boldsymbol{n}(1) \quad \cdots \quad \boldsymbol{n}(N)]$. In order to solve this problem, we consider the GLRT.

A. Derivation of the GLRT

In this section, we first derive the maximum-likelihood estimates (MLEs) of the unknown parameters under each hypothesis. The MLEs are then used to obtain the GLRT. Under the hypotheses made, the observations are Gaussian distributed, and the likelihood function is given by [2], [6]

$$\ell(\boldsymbol{Y}) = \frac{\exp\left\{-\frac{1}{\sigma^2}\sum_{t=1}^{N}\left\|\boldsymbol{y}(t) - \mu\boldsymbol{H}\boldsymbol{\theta}s(t) - \boldsymbol{A}\boldsymbol{u}(t)\right\|^2\right\}}{(\pi\sigma^2)^{mN}} \tag{3}$$

where $\mu = 0$ under H_0 and $\mu = 1$ under H_1. When σ^2 is unknown, its ML estimate is readily obtained as

$$\hat{\sigma}^2 = \frac{1}{mN}\sum_{t=1}^{N}\left\|\boldsymbol{y}(t) - \mu\boldsymbol{H}\boldsymbol{\theta}s(t) - \boldsymbol{A}\boldsymbol{u}(t)\right\|^2. \tag{4}$$

Reporting (4) in (3), it follows that the MLEs of $\boldsymbol{s}, \boldsymbol{U}$, and $\boldsymbol{\theta}$ are obtained by minimizing

$$\mathrm{Tr}\left\{\left(\boldsymbol{Y} - \mu\boldsymbol{H}\boldsymbol{\theta}\boldsymbol{s}^T - \boldsymbol{A}\boldsymbol{U}\right)\left(\boldsymbol{Y} - \mu\boldsymbol{H}\boldsymbol{\theta}\boldsymbol{s}^T - \boldsymbol{A}\boldsymbol{U}\right)^H\right\} \tag{5}$$

where $\mathrm{Tr}\{.\}$ stands for the trace of a matrix. At this stage, the problem is equivalent to that in [1], and we refer to [1] for details that will be omitted here. The matrix $\boldsymbol{U}$ that minimizes (5) is given by

$$\boldsymbol{U} = \left(\boldsymbol{A}^H\boldsymbol{A}\right)^{-1}\boldsymbol{A}^H\left(\boldsymbol{Y} - \mu\boldsymbol{H}\boldsymbol{\theta}\boldsymbol{s}^T\right). \tag{6}$$

Under H_0, all unknown parameters are estimated, and the MLE of σ^2 is

$$\hat{\sigma}_0^2 = \frac{1}{mN}\mathrm{Tr}\left\{\boldsymbol{P}_{\boldsymbol{A}}^{\perp}\boldsymbol{Y}\boldsymbol{Y}^H\right\} \tag{7}$$

where $\boldsymbol{P}_{\boldsymbol{A}}$ denotes the orthogonal projection onto $\langle \boldsymbol{A} \rangle$ and $\boldsymbol{P}_{\boldsymbol{A}}^{\perp} = \boldsymbol{I} - \boldsymbol{P}_{\boldsymbol{A}}$ the projection onto its orthogonal complement. Under H_1, inserting (6) in (5), one needs to minimize

$$\begin{aligned} &\mathrm{Tr}\left\{\left(\boldsymbol{Y} - \boldsymbol{H}\boldsymbol{\theta}\boldsymbol{s}^T\right)^H\boldsymbol{P}_{\boldsymbol{A}}^{\perp}\left(\boldsymbol{Y} - \boldsymbol{H}\boldsymbol{\theta}\boldsymbol{s}^T\right)\right\} \\ &= \left(\boldsymbol{\theta}^H\boldsymbol{H}^H\boldsymbol{P}_{\boldsymbol{A}}^{\perp}\boldsymbol{H}\boldsymbol{\theta}\right)\left\|\boldsymbol{s}^* - \frac{\boldsymbol{Y}^H\boldsymbol{P}_{\boldsymbol{A}}^{\perp}\boldsymbol{H}\boldsymbol{\theta}}{\boldsymbol{\theta}^H\boldsymbol{H}^H\boldsymbol{P}_{\boldsymbol{A}}^{\perp}\boldsymbol{H}\boldsymbol{\theta}}\right\|^2 \\ &\quad + \mathrm{Tr}\left\{\boldsymbol{P}_{\boldsymbol{A}}^{\perp}\boldsymbol{Y}\boldsymbol{Y}^H\right\} - \frac{\boldsymbol{\theta}^H\boldsymbol{H}^H\boldsymbol{P}_{\boldsymbol{A}}^{\perp}\boldsymbol{Y}\boldsymbol{Y}^H\boldsymbol{P}_{\boldsymbol{A}}^{\perp}\boldsymbol{H}\boldsymbol{\theta}}{\boldsymbol{\theta}^H\boldsymbol{H}^H\boldsymbol{P}_{\boldsymbol{A}}^{\perp}\boldsymbol{H}\boldsymbol{\theta}}. \end{aligned} \tag{8}$$

The MLE of $\boldsymbol{\theta}$ is thus given, up to a scaling factor, by the principal eigenvector of $\left(\boldsymbol{G}^H\boldsymbol{G}\right)^{-1}\boldsymbol{G}^H\boldsymbol{Y}\boldsymbol{Y}^H\boldsymbol{G}$ with $\boldsymbol{G} = \boldsymbol{P}_{\boldsymbol{A}}^{\perp}\boldsymbol{H}$. The subspace

$\langle \boldsymbol{G} \rangle$ corresponds to the part of $\langle \boldsymbol{H} \rangle$ in $\langle \boldsymbol{A} \rangle^{\perp}$. The noise power estimate under H_1 is

$$\widehat{\sigma}_1^2 = \frac{1}{mN}\left[\mathrm{Tr}\left\{\boldsymbol{P}_{\boldsymbol{A}}^{\perp}\boldsymbol{Y}\boldsymbol{Y}^H\right\} - \lambda_{\max}\left\{\boldsymbol{P}_{\boldsymbol{G}}\boldsymbol{Y}\boldsymbol{Y}^H\right\}\right] \tag{9}$$

where $\lambda_{\max}\{.\}$ is the largest eigenvalue of the matrix between braces. Therefore, the mN-root generalized-likelihood ratio (GLR) can be obtained as

$$\begin{aligned} M_2(\boldsymbol{Y}) &= \left[\frac{\widehat{\ell}(\boldsymbol{Y}|H_1)}{\widehat{\ell}(\boldsymbol{Y}|H_0)}\right]^{1/mN} = \frac{\widehat{\sigma}_0^2}{\widehat{\sigma}_1^2} \\ &= \frac{\mathrm{Tr}\left\{\boldsymbol{P}_{\boldsymbol{A}}^{\perp}\boldsymbol{Y}\boldsymbol{Y}^H\right\}}{\mathrm{Tr}\left\{\boldsymbol{P}_{\boldsymbol{A}}^{\perp}\boldsymbol{Y}\boldsymbol{Y}^H\right\} - \lambda_{\max}\left\{\boldsymbol{P}_{\boldsymbol{G}}\boldsymbol{Y}\boldsymbol{Y}^H\right\}}. \end{aligned} \tag{10}$$

When $M_2(\boldsymbol{Y})$ is above some threshold, H_1 is decided to hold. The detector operates in $\langle A \rangle^{\perp}$: there, it compares the energy of the most energetic component due to $\langle \boldsymbol{H} \rangle$ to the total energy in $\langle \boldsymbol{A} \rangle^{\perp}$. Note that $M_2(\boldsymbol{Y})$ is invariant to transformations that rotate $\boldsymbol{Y}$ within $\langle \boldsymbol{G} \rangle$ and to scaling. When σ^2 is known, the GLR is given by [1]

$$\boxed{L_1(\boldsymbol{Y}) = \sigma^{-2}\lambda_{\max}\left\{\boldsymbol{P}_{\boldsymbol{G}}\boldsymbol{Y}\boldsymbol{Y}^H\right\}.} \tag{11}$$

Observe that $M_2(\boldsymbol{Y})$ may also be replaced by the monotone function $1 - M_2^{-1}(\boldsymbol{Y})$, which is

$$\boxed{L_2(\boldsymbol{Y}) = 1 - \frac{1}{M_2(\boldsymbol{Y})} = \frac{\lambda_{\max}\left\{\boldsymbol{P}_{\boldsymbol{G}}\boldsymbol{Y}\boldsymbol{Y}^H\right\}}{\mathrm{Tr}\left\{\boldsymbol{P}_{\boldsymbol{A}}^{\perp}\boldsymbol{Y}\boldsymbol{Y}^H\right\}}.} \tag{12}$$

Thus, the known σ^2 in (11) is replaced by $\mathrm{Tr}\left\{\boldsymbol{P}_{\boldsymbol{A}}^{\perp}\boldsymbol{Y}\boldsymbol{Y}^H\right\}$, which is, within a factor $1/mN$, the MLE of σ^2 under H_0 (see (7)).

Remark 1: In the single-snapshot case, $\boldsymbol{Y} = \boldsymbol{y}$ is an $L|1$ vector, and the GLR in (10) reduces to

$$M_2(\boldsymbol{y}) = \frac{\boldsymbol{y}^H\boldsymbol{P}_{\boldsymbol{A}}^{\perp}\boldsymbol{y}}{\boldsymbol{y}^H\left(\boldsymbol{P}_{\boldsymbol{A}}^{\perp} - \boldsymbol{P}_{\boldsymbol{G}}\right)\boldsymbol{y}} = \frac{\boldsymbol{y}^H\boldsymbol{P}_{\boldsymbol{A}}^{\perp}\boldsymbol{y}}{\boldsymbol{y}^H\boldsymbol{P}_{\boldsymbol{A}}^{\perp}\boldsymbol{P}_{\boldsymbol{G}}^{\perp}\boldsymbol{P}_{\boldsymbol{A}}^{\perp}\boldsymbol{y}}$$

where, to obtain the second equality, we made use of [3, eq. (3.4)–(3.7)]. Furthermore, using the fact that $\boldsymbol{P}_{\boldsymbol{G}} = \boldsymbol{P}_{\boldsymbol{A}}^{\perp}\boldsymbol{P}_{\boldsymbol{G}}\boldsymbol{P}_{\boldsymbol{A}}^{\perp}$, it follows that the GLRT consists of comparing

$$M_2(\boldsymbol{y}) - 1 = \frac{\boldsymbol{y}^H\boldsymbol{P}_{\boldsymbol{A}}^{\perp}\boldsymbol{P}_{\boldsymbol{G}}\boldsymbol{P}_{\boldsymbol{A}}^{\perp}\boldsymbol{y}}{\boldsymbol{y}^H\boldsymbol{P}_{\boldsymbol{A}}^{\perp}\boldsymbol{P}_{\boldsymbol{G}}^{\perp}\boldsymbol{P}_{\boldsymbol{A}}^{\perp}\boldsymbol{y}} \tag{13}$$

to a threshold. The previous equation is the GLR for detecting a subspace signal in subspace interference and noise of unknown level when a single snapshot is available (see [3, eq. (8.2)]). Note that $M_2(\boldsymbol{y}) - 1$ is the ratio of two chi-squared distributed random variables with $r = p$ and $q = L - J - p$ degrees of freedom, respectively. Therefore, it follows an F-distribution [2]. Accordingly, when $p = 1$, i.e., when there is no uncertainty about the steering vector of interest, $\boldsymbol{G} = \boldsymbol{P}_{\boldsymbol{A}}^{\perp}\boldsymbol{h} = \boldsymbol{g}$ is a vector and $\boldsymbol{P}_{\boldsymbol{G}}\boldsymbol{Y}\boldsymbol{Y}^H$ has a single eigenvalue. In this case

$$M_2(\boldsymbol{Y}) - 1 = \frac{\mathrm{Tr}\left\{\boldsymbol{P}_{\boldsymbol{A}}^{\perp}\boldsymbol{P}_{\boldsymbol{G}}\boldsymbol{P}_{\boldsymbol{A}}^{\perp}\boldsymbol{Y}\boldsymbol{Y}^H\right\}}{\mathrm{Tr}\left\{\boldsymbol{P}_{\boldsymbol{A}}^{\perp}\boldsymbol{P}_{\boldsymbol{G}}^{\perp}\boldsymbol{P}_{\boldsymbol{A}}^{\perp}\boldsymbol{Y}\boldsymbol{Y}^H\right\}} \tag{14}$$

is now the ratio of two chi-squared distributed random variables with $r = N$ and $q = N(L - J - 1)$ degrees of freedom, respectively. When $N = 1$, it reduces to the GLRT for detecting a known signal in subspace interference and noise of unknown level (see [3, equation (6.4)]).

B. Distribution of the GLR Under the Null Hypothesis

In order to set the threshold η of the test for a given probability of false alarm P_{FA}, we need to derive the probability density function (pdf) of the GLR under the null hypothesis. Although the derivation of the GLR for unknown σ^2 is a straightforward extension of the GLR with known σ^2, it turns out that the derivation of its pdf is much more complicated in the present case, as is illustrated now. In order to obtain this pdf, we will write the GLR in a canonical from, i.e., as a function of independent random variables. To do so, let

$$\boldsymbol{U}_{\boldsymbol{A}}^{\perp} = \begin{bmatrix} \underset{L|p}{\boldsymbol{U}_G} & \underset{L|L-J-p}{\boldsymbol{U}_2} \end{bmatrix} \tag{15}$$

denote an orthonormal basis for $\left\langle \boldsymbol{A}^{\perp} \right\rangle$, where $\boldsymbol{U}_G \in \mathbb{C}^{L\times p}$ is a unitary basis for $\langle \boldsymbol{G} \rangle$ and $\boldsymbol{U}_2 \in \mathbb{C}^{L\times L-J-p}$ is a unitary basis for the complement of $\langle \boldsymbol{G} \rangle$ in $\left\langle \boldsymbol{A}^{\perp} \right\rangle$, i.e., a unitary basis for $\left\langle \boldsymbol{P}_{\boldsymbol{A}}^{\perp}\boldsymbol{P}_{\boldsymbol{G}}^{\perp}\boldsymbol{P}_{\boldsymbol{A}}^{\perp} \right\rangle$. First, note that under H_0

$$\begin{aligned} \boldsymbol{P}_{\boldsymbol{A}}^{\perp}\boldsymbol{Y}\boldsymbol{Y}^H &= \boldsymbol{U}_{\boldsymbol{A}}^{\perp}\boldsymbol{U}_{\boldsymbol{A}}^{\perp H}\boldsymbol{Y}\boldsymbol{Y}^H = \boldsymbol{U}_{\boldsymbol{A}}^{\perp}\boldsymbol{U}_{\boldsymbol{A}}^{\perp H}\boldsymbol{N}\boldsymbol{N}^H \\ &= \boldsymbol{U}_G\boldsymbol{U}_G^H\boldsymbol{N}\boldsymbol{N}^H + \boldsymbol{U}_2\boldsymbol{U}_2^H\boldsymbol{N}\boldsymbol{N}^H \end{aligned} \tag{16}$$

so that

$$\mathrm{Tr}\left\{\boldsymbol{P}_{\boldsymbol{A}}^{\perp}\boldsymbol{Y}\boldsymbol{Y}^H\right\} = \mathrm{Tr}\left\{\boldsymbol{N}_G\boldsymbol{N}_G^H\right\} + \mathrm{Tr}\left\{\boldsymbol{N}_2\boldsymbol{N}_2^H\right\} \tag{17a}$$

$$\lambda_{\max}\left\{\boldsymbol{P}_{\boldsymbol{G}}\boldsymbol{Y}\boldsymbol{Y}^H\right\} = \lambda_{\max}\left\{\boldsymbol{N}_G\boldsymbol{N}_G^H\right\} \tag{17b}$$

where $\boldsymbol{N}_G = \boldsymbol{U}_G^H\boldsymbol{N}$ [respectively, $\boldsymbol{N}_2 = \boldsymbol{U}_2^H\boldsymbol{N}$] is a $p \times N$ [respectively, a $L-J-p\times N$] matrix whose columns are independent p-variate [respectively, $L - J - p$-variate] complex Gaussian vectors with covariance matrix $\sigma^2\boldsymbol{I}$. Furthermore, $\boldsymbol{N}_G$ and $\boldsymbol{N}_2$ are uncorrelated and hence independent.

Let us define $m = \min(p, N)$, $M = \max(p, N)$, and let us denote by $\lambda_1 > \lambda_2 > \cdots > \lambda_m \geq 0$ the first m eigenvalues of $\boldsymbol{W}_G = \boldsymbol{N}_G\boldsymbol{N}_G^H$. Accordingly, let us denote

$$t_2 = \mathrm{Tr}\left\{\boldsymbol{N}_2\boldsymbol{N}_2^H\right\};\ t = \mathrm{Tr}\left\{\boldsymbol{N}_G\boldsymbol{N}_G^H\right\} = \sum_{k=1}^{m}\lambda_k. \tag{18}$$

Then, $M_2(\boldsymbol{Y})$ can be rewritten as

$$M_2(\boldsymbol{Y}) = \frac{\sum_{k=1}^{m}\lambda_k + t_2}{\sum_{k=2}^{m}\lambda_k + t_2} = \frac{t + t_2}{t - \lambda_1 + t_2}. \tag{19}$$

From inspection of (19), it is clear that the GLR is invariant to scaling in $\boldsymbol{N}$ and is thus CFAR with respect to the noise level σ^2. Without loss of generality, we assume in the sequel that the columns of $\boldsymbol{N}$ are independent complex Gaussian vectors with covariance matrix $\boldsymbol{I}$. As will become clearer below, it is more convenient to consider

$$\begin{aligned} L_2(\boldsymbol{Y}) &= \frac{M_2(\boldsymbol{Y}) - 1}{M_2(\boldsymbol{Y})} = \frac{\lambda_1}{t + t_2} \\ &= \frac{\frac{\lambda_1}{t}}{1 + \frac{t_2}{t}} = \frac{a}{1 + f} = ab \end{aligned} \tag{20}$$

instead of $M_2(\boldsymbol{Y})$ since $a = \lambda_1/t$ and $b = (1 + t_2/t)^{-1}$ are independent random variables, as will be shown next. First, we derive the pdf of b. It is well known [7] that t_2 has a central chi-squared distribution with $q = N(L - J - p)$ degrees of freedom. Accordingly, t has a central chi-squared distribution with $r = pN$ degrees of freedom. The pdf's of t_2 and t are thus given by

$$f_{T_2}(t_2) = \frac{1}{\Gamma(q)} e^{-t_2} t_2^{q-1}, \qquad t_2 \geq 0$$
$$f_T(t) = \frac{1}{\Gamma(r)} e^{-t} t^{r-1}, \qquad t \geq 0. \tag{21}$$

Therefore, $b = t/(t + t_2) = 1/(1 + f)$ has a beta distribution

$$f_B(b) = \frac{\Gamma(q+r)}{\Gamma(q)\Gamma(r)} b^{r-1}(1-b)^{q-1}, \qquad 0 \leq b \leq 1. \tag{22}$$

Next, we show that a is independent of t and hence of b. Since $\boldsymbol{W}_G = \boldsymbol{N}_G \boldsymbol{N}_G^H$ has a complex Wishart distribution $CW_p(N, \boldsymbol{I})$, the joint pdf of its eigenvalues is given by [8], [9]

$$f_{\Lambda_1,\Lambda_2,\ldots,\Lambda_m}(\lambda_1, \lambda_2, \ldots, \lambda_m) = c \exp\left\{-\sum_{k=1}^{m} \lambda_k\right\} \left(\prod_{k=1}^{m} \lambda_k^{M-m}\right) \left(\prod_{1 \leq k < \ell \leq m} (\lambda_k - \lambda_\ell)^2\right) \tag{23}$$

where $c^{-1} = \prod_{k=1}^{m} \Gamma(m-k+1)\Gamma(M-k+1)$. Let us make the change of variables from $\{\lambda_k\}_{k=1}^{m}$ to $z_0 = t, z_1, \ldots, z_{m-1}$, where

$$z_k = \frac{\lambda_k}{t}, \quad k = 1, \ldots, m;\ z_1 = \frac{\lambda_1}{t} = a.$$

Note that $\sum_{k=1}^{m} z_k = 1$ and hence $z_m = 1 - \sum_{k=1}^{m-1} z_k$. The Jacobian of the transformation is easily seen to be t^{m-1}. Therefore, the joint density function of $z_0 = t, z_1 = a, z_2, \ldots, z_{m-1}$ factors as

$$\left[\frac{1}{\Gamma(mM)} t^{mM-1} e^{-t}\right] \times \left[c\Gamma(mM) \left(\prod_{k=1}^{m} z_k^{M-m}\right) \left(\prod_{1 \leq k < \ell \leq m} (z_k - z_\ell)^2\right)\right]$$

which shows that t is independent of $z_1, \ldots, z_{m-1}$ and hence of $a = z_1$. Moreover, we find that t is χ^2_{mN} distributed. The pdf of z_1 could in principle be obtained as

$$f_{Z_1}(z_1) = c\Gamma(pN) \int \cdots \int \prod_{k=1}^{m} z_k^{M-m} \prod_{1 \leq k < \ell \leq m} (z_k - z_\ell)^2 dz_2 \cdots dz_{m-1} \tag{24}$$

where the integration is over the domain $0 \leq z_m < z_{m-1} < \cdots < z_1 \leq 1$ and $z_m + z_{m-1} + \cdots + z_1 = 1$. However, it appears quite complicated to obtain a closed-form expression for this integral for any p. Indeed, it seems that there does not exist in the literature a closed-form and simple expression for the pdf of a for any value of p. However, for the problem at hand, p is the dimension of the subspace, where $\boldsymbol{a}$ is expected to lie. Hence, p is typically small; otherwise, we have a very poor knowledge of the steering vector that the beamformer attempts to recover, which is contrary to common sense. Furthermore, as was illustrated in [1], choosing $p > 2$ does not result in any detection performance improvement, and hence the choice $p = 2$ or $p = 3$ appears to be the most appropriate. In the sequel, we derive closed-form expressions for the pdf of a in the cases $p = 2$ and $p = 3$. We consider now that $N \geq p$: the case $N = 1$ is studied in [3], and considering $p = 3$, $N = 2$ is equivalent to considering $N = 3$, $p = 2$ by interchanging p and N in the expressions.

When $p = 2$, there is no integral in (24) and the pdf of a simply writes

$$f_A(a) = c\, \Gamma(2N) a^{N-2} (1-a)^{N-2} (2a-1)^2, \quad \frac{1}{2} \leq a \leq 1. \tag{25}$$

In this case, it is also possible to show that the nth-order moment of a is given by

$$\mathcal{E}\{a^n\} = \frac{\Gamma(2N)}{2^{2N-2+n}\Gamma(N)} \times \sum_{k=0}^{n} \frac{\Gamma\left(\frac{k+3}{2}\right)}{\Gamma(k+1)\Gamma(n-k+1)\Gamma\left(N + \frac{k+1}{2}\right)}. \tag{26}$$

When $p = 3$, we need to integrate the function in (24) over the variable z_2. Doing so, it can be shown that (for the sake of brevity, the detailed derivations are omitted) the pdf of a is given by

$$\begin{aligned} f_A(a) = c_1\, &(1-a)^{2N+1} a^{N-3} \\ &\times \Big\{ \left[(2N+1)(2N-1)h^2(a) - 6(2N+1)h(a) + 15\right] \\ &\times B_{z(a)}\left(\frac{3}{2}, N-2\right) + [1 - z(a)]^{N-2} z^{3/2}(a) \\ &\times \left[2(2N+3)z^2(a) - 10\right] \Big\}, \qquad \frac{1}{3} \leq a \leq 1 \end{aligned} \tag{27}$$

where $c_1 = c\,\Gamma(3N)/2^{2N}(2N+1)(2N-1)$, $h(a) = ((3a-1)/(1-a))^2$, $z(a) = \min(1, h(a))$ and $B_z(a,b)$ is the incomplete Beta function [10].

The pdf of $g = L_2(\boldsymbol{Y}) = ab$ is thus given by

$$f_G(g) = \int f_A(a) f_B\left(\frac{g}{a}\right) \frac{da}{a} = \int f_A\left(\frac{g}{b}\right) f_B(b) \frac{db}{b} \tag{28}$$

where $f_B(.)$ is given by (22) and $f_A(.)$ is given by (25) when $p = 2$ and (27) when $p = 3$. In the case $p = 2$, the integral reduces to

$$\begin{aligned} f_G(g) &= c_2 g^{r-1} \int_{\max(g,1/2)}^{1} z^{N-q-r-1} (1-z)^{N-2} (2z-1)^2 (z-g)^{q-1} dz \\ &= c_2 g^{N-2} \int_{g}^{\min(1,2g)} (1-z)^{q-1} (2g-z)^2 (z-g)^{N-2} dz. \end{aligned} \tag{29}$$

For illustration purposes, Fig. 1 displays (29) for various N, when $L = 10$, $J = 2$, and $p = 2$. It can be observed that the mean of $f_G(g)$ decreases as N increases and that the tail probabilities of $f_G(g)$ decrease more rapidly as N increases.

III. Numerical Illustrations

In this section, we illustrate the performance of the CFAR-GLRT detector and compare it with the performance of the GLRT for known noise level. Similarly to [1], we consider a uniform linear array of $L = 10$ sensors spaced a half-wavelength apart. We consider the case of a Ricean channel for which the steering vector can be written as [11]

$$\boldsymbol{a} = \boldsymbol{a}_0 + \frac{1}{\sqrt{q}} \sum_{k=1}^{q} g_k \boldsymbol{a}(\phi_k) \tag{30}$$

where $\boldsymbol{a}_0$ corresponds to the line-of-sight component, and the second term in the right-hand side of (30) stands for the contribution of scatterers. The g_k are zero-mean, independent, and identically distributed

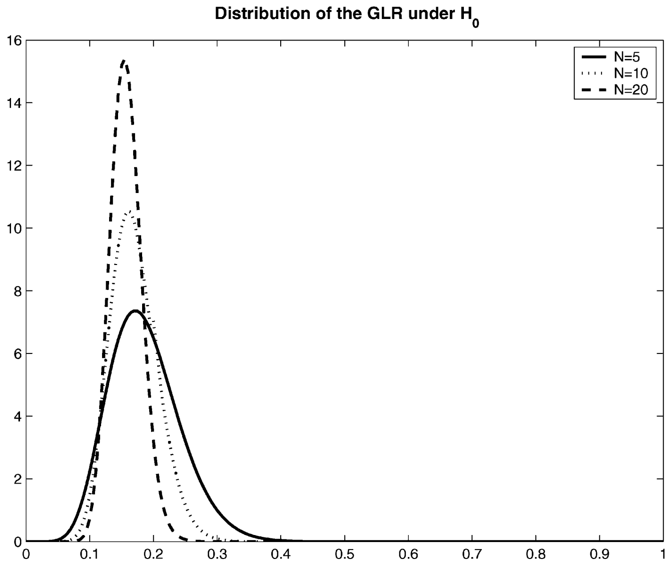

Fig. 1. Distribution of the GLR for $N = 5, 10, 20$. $L = 10$, $J = 2$, and $p = 2$.

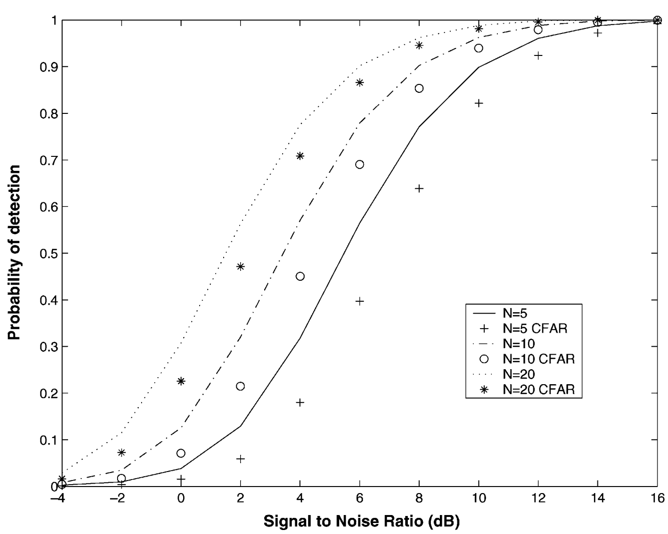

Fig. 2. Probability of detection versus SNR. $\boldsymbol{a} \in \langle \boldsymbol{H} \rangle$. UR $= -6$ dB and $P_{\mathrm{FA}} = 10^{-4}$.

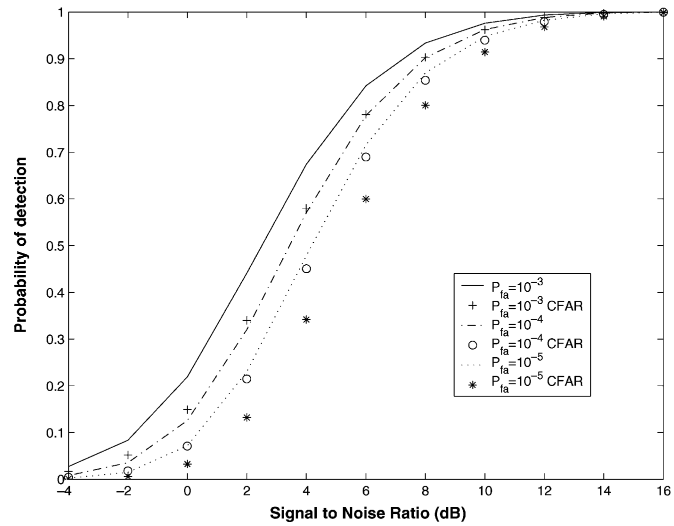

Fig. 3. Probability of detection versus SNR. $\boldsymbol{a} \in \langle \boldsymbol{H} \rangle$. UR $= -6$ dB and $N = 10$.

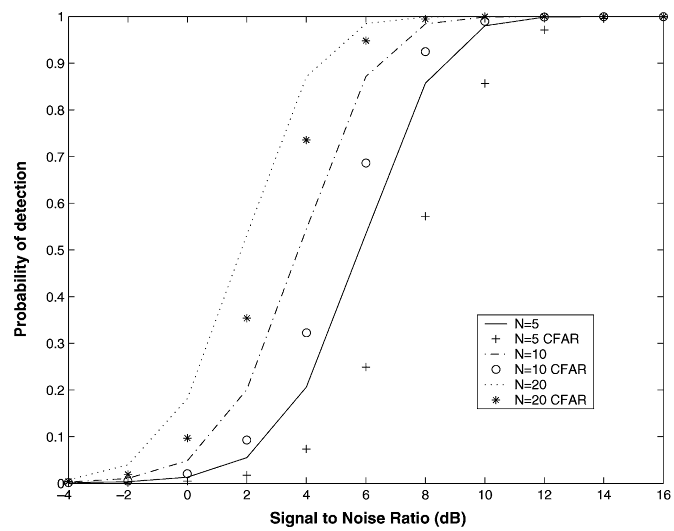

Fig. 4. Probability of detection versus SNR. UR $= -6$ dB and $P_{\mathrm{FA}} = 10^{-4}$.

random variables with power σ_g^2, and ϕ_k are independent random variables with pdf $p(\phi)$. The covariance matrix of the steering vector errors is given by [11]

$$\boldsymbol{C}_a = \sigma_g^2 \int \boldsymbol{a}(\phi)\boldsymbol{a}^H(\phi)p(\phi)\, d\phi. \tag{31}$$

When the angular spread of the scatterers is small, it is known that $\boldsymbol{C}_a$ has only a few significant eigenvalues; hence, subspace modeling of the steering vector becomes relevant. In the sequel, the actual steering vector is generated as

$$\boldsymbol{a} = \boldsymbol{a}_0 + \alpha \boldsymbol{u}_1 \tag{32}$$

where $\boldsymbol{a}_0 = \boldsymbol{a}(0^\circ)$ is the line-of-sight component, and $\boldsymbol{u}_1$ is the principal eigenvector of $\boldsymbol{C}_a$: hence, $p = 2$ and $\boldsymbol{H} = [\, \boldsymbol{a} \quad \boldsymbol{u}_1 \,]$. α is drawn from a proper complex-valued multivariate normal distribution with zero-mean and variance σ_α^2. In the simulations, we assume a Gaussian distribution for the scatterers with standard deviation $\sigma_\theta = 15^\circ$. We define the uncertainty ratio (UR) and the (array) signal-to-noise ratio (SNR) as

$$\mathrm{UR} = 10 \log_{10} \left(\frac{\sigma_\alpha^2}{\boldsymbol{a}_0^H \boldsymbol{a}_0} \right) \tag{33}$$

$$\mathrm{SNR} = 10 \log_{10} \left(\frac{P \left[\boldsymbol{a}_0^H \boldsymbol{a}_0 + \sigma_\alpha^2 \right]}{\sigma^2} \right) \tag{34}$$

where P is the power for the signal of interest. Finally, we assume that $J = 2$ interferences present, with DOAs -20°, 30° and powers 20 and 30 dB above the white noise level, respectively.

For each figure, one million Monte Carlo simulations are run with a different $\boldsymbol{a}$ drawn from (32); this enables us to characterize the average behavior of the GLRTs. In Figs. 2 and 3, we display the probability of detection for various number of snapshots N and various P_{FA}, respectively. It can be observed that the CFAR-GLRT incurs only a 1-dB loss compared with the GLRT for known noise level, which is not an important price to be paid given that we need not know the noise level.

Finally, we test the robustness of the detector when $\boldsymbol{a}$ is generated as in (30). In such a case, $\boldsymbol{a}$ does not belong to a subspace since $\boldsymbol{C}_a$ is full rank. However, the GLRT detectors are used with

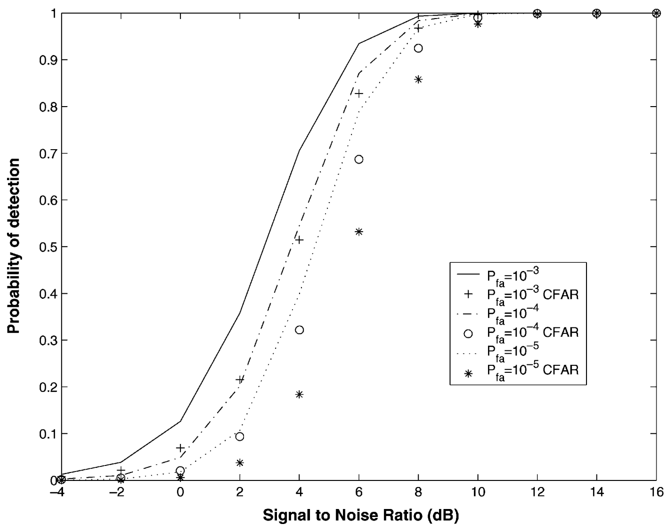

Fig. 5. Probability of detection versus SNR. UR $= -6$ dB and $N = 10$.

the assumption that $\boldsymbol{a}$ is generated as in (32). In this case, UR and SNR are defined as UR $= 10\log_{10}\left(\mathrm{Tr}\left\{\boldsymbol{C}_a\right\}/\boldsymbol{a}_0^H\boldsymbol{a}_0\right)$ and SNR $= 10\log_{10}\left(P\left[\boldsymbol{a}_0^H\boldsymbol{a}_0 + \mathrm{Tr}\left\{\boldsymbol{C}_a\right\}\right]/\sigma^2\right)$. The detection performance is plotted in Figs. 4 and 5. Despite the fact that $\boldsymbol{a}$ does not belong to $\langle\boldsymbol{H}\rangle$, the detection performance is not affected, and hence the detection scheme turns out to be rather robust.

IV. Conclusion

In this correspondence, we considered the problem of detecting a signal whose spatial signature is unknown but known to lie in a given linear subspace, in the presence of interferences and broadband noise. We have extended the results of [1] to the case of unknown noise level and derived the GLRT, which is CFAR with respect to the noise level. We showed that the GLRT detector involves the ratio of the largest eigenvalue of a complex Wishart matrix to its trace whereas, in the known noise level case, it involved the largest eigenvalue only. The distribution of the GLR was derived under the null hypothesis. Simulation results indicate that there is a 1-dB loss between the GLRT with known σ^2 and the CFAR-GLRT with unknown σ^2. Furthermore, the detection test was shown to be rather robust when the spatial signature does not completely belong to a subspace.

References

[1] O. Besson, L. L. Scharf, and F. Vincent, "Matched direction detectors and estimators for array processing with subspace steering vector uncertainties," *IEEE Trans. Signal Process.*, vol. 53, no. 12, pp. 4453–4463, Dec. 2005.

[2] L. L. Scharf, *Statistical Signal Processing: Detection, Estimation and Time Series Analysis*. Reading, MA: Addison-Wesley, 1991.

[3] L. L. Scharf and B. Friedlander, "Matched subspace detectors," *IEEE Trans. Signal Process.*, vol. 42, no. 8, pp. 2146–2157, Aug. 1994.

[4] S. Kraut, L. L. Scharf, and T. McWhorter, "Adaptive subspace detectors," *IEEE Trans. Signal Process.*, vol. 49, no. 1, pp. 1–16, Jan. 2001.

[5] L. L. Scharf and M. McCloud, "Blind adaptation of zero forcing projections and oblique pseudo-inverses for subspace detection and estimation when interference dominates noise," *IEEE Trans. Signal Process.*, vol. 50, no. 12, pp. 2938–2946, Dec. 2002.

[6] S. Kay, *Fundamentals of Statistical Signal Processing: Estimation Theory*. Englewood Cliffs, NJ: Prentice-Hall, 1993.

[7] R. Muirhead, *Aspects of Multivariate Statistical Theory*. New York: John Wiley, 1982.

[8] A. James, "Distributions of matrix variates and latent roots derived from normal samples," *Ann. Mathemat. Stat.*, vol. 35, pp. 475–501, Jun. 1964.

[9] M. Kang and M.-S. Alouini, "Largest eigenvalue of complex Wishart matrices and performance analysis of MIMO MRC systems," *IEEE J. Sel. Areas Commun.*, vol. 21, no. 3, pp. 418–426, Apr. 2003.

[10] *Handbook of Mathematical Functions with Formulas, Graphs, and Mathematical Tables*, M. Abramowitz and I. Stegun, Eds., Dover , New York, 1970.

[11] G. Fuks, J. Goldberg, and H. Messer, "Bearing estimation in a ricean channel-Part I: Inherent accuracy limitations," *IEEE Trans. Signal Process.*, vol. 49, no. 5, pp. 925–937, May 2001.

Equalization of a MIMO Channel Using FIR Inverses

K. Deergha Rao, *Senior Member, IEEE*

***Abstract*—In the modern method of equalization, the problem of multiple-input multiple-output (MIMO) finite-impulse-response (FIR) channel equalization boils down to finding the MIMO FIR inverses. This correspondence proposes and proves a theorem that states the condition for the existence of these inverses, which are also FIR. A numerical example is provided to illustrate how the FIR inverses can be evaluated and used for equalization of a channel with known channel parameters.**

***Index Terms*—Equalization, finite-impulse-response (FIR) inverses, multiple-input multiple-output (MIMO) channel, multiuser system.**

I. Introduction

Users in a wireless network share a common medium, and their transmissions may interfere with one another. A general model of a multiuser communication system is the multiple-input multiple-output (MIMO) channel, as shown in Fig. 1. Here $x_i(n)$ are transmitted signals from M users, $y_i(n)$ are the received signals at N sensors, which can be antenna-array elements or virtual receivers of temporal processing [1, vol. 1, ch. 8]. The number of sensors (N) must be at least equal to the number of source signals (M). The basic channel equalization problem is to design an estimator, such that multiple sources are extracted in an optimal fashion. It is unrealistic to assume that the receiver knows the channel parameters in a wireless mobile network. Considerable research has been devoted to estimation of channel parameters [2]–[4].

Generally, the data and channel responses may be represented as polynomials in the z-transform domain, and the implementations are restricted to MIMO polynomial finite-impulse-response (FIR) filter. Here, a theorem is proposed and proved for finding the inverse of the MIMO FIR filter such that the inverse is also FIR. An example illustrates channel equalization with known channel parameters.

This correspondence is organized as follows. The channel model is described in Section II. In Section III, a theorem is proposed and proved for finding the inverse of the MIMO FIR filter such that the inverse is also FIR and illustrated for channel equalization with known channel and Section IV contains the conclusions.

Manuscript received May 24, 2005; revised August 14, 2005. The associate editor coordinating the review of this manuscript and approving it for publication was Prof. Yuri I. Abramovich.

The author is with the Research and Training Unit For Navigational Electronics, Osmania University, Hyderabad 500 007, India (e-mail: korraidrao@yahoo.com).

Digital Object Identifier 10.1109/TSP.2006.874793